Electronic Supplementary Material (ESI) for Journal of Materials Chemistry C.
This journal is © The Royal Society of Chemistry 2017

Altering Polarization Attributes in Ferroelectric Metallo-Cavitands by Varying Hydrated Alkali-Metal Guest Cations

Anant Kumar Srivastava,[a] Thangavel Vijayakanth,[a] Pillutla Divya,[c] B. Praveenkumar,*[c] Alexander Steiner*[d] and Ramamoorthy Boomishankar*[a,b]

[a] Department of Chemistry, Indian Institute of Science Education and Research (IISER), Pune, Dr. Homi Bhabha Road, Pune-411008, India.

[b] Centre for Energy Science, Indian Institute of Science Education and Research (IISER), Pune, Dr. Homi Bhabha Road, Pune-411008, India.

[c]Armament Research and Development Establishment, Dr. Homi Bhabha Road, Pune – 411021, India.

[d] Department of Chemistry, University of Liverpool, Crown Street, Liverpool – L69 7ZD, United Kingdom.

Supplementary Information

Experimental Section

General Remarks

All manipulations involving phosphorus halides were performed under a dry nitrogen atmosphere in standard Schlenk-glassware; toluene was dried over sodium. The ligand L was synthesized as per our reported procedure.[1] $Ni(NO_3)_2\cdot 6H_2O$ and $Co(NO_3)_2\cdot 6H_2O$ were purchased from Merck and used as received. KNO_3, $NaNO_3$, and $RbNO_3$ were purchased from Sigma-Aldrich, while $LiNO_3$ and $CsNO_3$ were locally purchased and used as received. The X-ray powder diffraction (PXRD) data were obtained from a Bruker-D8 Advance diffractometer. FT-IR in attenuated total reflectance (ATR) mode was taken on neat samples on a Bruker Alpha spectrophotometer. Elemental analyses were performed on a Vario-EL cube elemental analyzer.

Syntheses

L: Ligand was synthesized as per the known procedure[1] and was then subjected to react with $Ni(NO_3)_2\cdot 6H_2O$ and $Co(NO_3)_2\cdot 6H_2O$ in absence/ presence of alkali metal salts.

$[\{Ni_4L_8(H_2O)_8\}\supset 9(H_2O)]\cdot(NO_3)_8\cdot 25(H_2O)$ (1): To a stirred solution of L (62 mg, 0.2 mmol) in MeOH (4ml), $Ni(NO_3)_2\cdot 6H_2O$ (30 mg, 0.1 mmol) in H_2O (2ml) was added. The mixture was subjected to continuous stirring for an hour. Then the solution was filtered through a thick pad of celite, and the filtrate was left undisturbed at room temperature for crystallization. The blue coloured single crystals of **1** suitable for SCXRD analysis were obtained after 2-3 weeks. Yield: 61% (61 mg), based on Ni. FT-IR data (cm^{-1}): 3744, 3124, 2961, 1646, 1582, 1504, 1476, 1394, 1327, 1268, 1184, 1117, 1058, 1031, 945, 806, 748, 694. Anal. Calcd. for $C_{128}H_{204}N_{40}O_{74}P_8Ni_4$: C, 38.73; H, 5.18; N, 14.11. Found: C, 39.01; H, 4.95; N, 14.12.

$[\{Co_4L_8(H_2O)_8\}\supset 9(H_2O)]\cdot(NO_3)_8\cdot 27(H_2O)$ (2): The similar procedure, as stated above for **1**, was adopted by using $Co(NO_3)_2\cdot 6H_2O$ (29 mg, 0.1 mmol) in place of $Ni(NO_3)_2\cdot 6H_2O$. The orange coloured single crystals of **2** suitable for SCXRD analysis were obtained after 2-3 weeks. Yield: 9% (9 mg), based on Co. FT-IR data (cm^{-1}): 3746, 3132, 2959, 1648, 1580, 1506, 1475, 1391, 1326, 1268, 1180, 1117, 1050, 1029, 949, 808, 749, 694. Anal. Calcd. for $C_{128}H_{208}N_{40}O_{76}P_8Co_4$: C, 38.37; H, 5.23; N, 13.98. Found: C, 38.59; H, 4.91; N, 14.15.

Synthesis of [Hy-A]$\subset$1 and [Hy-A]$\subset$2 host-guest systems (where A= Li^+, Na^+, K^+, Rb^+, Cs^+ ions): The [Hy-A]$\subset$**1** and [Hy-A]$\subset$**2** systems were synthesized by adopting the following procedure:

(a) To a stirred solution of L (62 mg, 0.2 mmol) in MeOH (5ml), $Ni(NO_3)_2\cdot 6H_2O$/ $Co(NO_3)_2\cdot 6H_2O$ (0.1 mmol) and ANO_3 (0.1 mmol) in H_2O (3ml) were added and stirred further.

The solution was then filtered through a thick pad of celite and left for crystallization. Definite shaped crystals of [Hy-A]⊂**1** or [Hy-A]⊂**2** suitable for SCXRD analysis were obtained after 10-15 days.

(b) To a solution of ANO_3 (1 mmol) in methanol (4 ml) and water (4 ml), crystals of **1** or **2** (20 mg) were added and stirred for 24 hours. The solution was then filtered through a thick pad of celite and left for crystallization. Definite shaped single crystals suitable for SCXRD analysis were obtained after 2-3 weeks.

Characterization data for [Hy-A]⊂1 and [Hy-A]⊂2 systems (reported yields are based on method a):

$[\{Ni_4L_8(H_2O_8\}\supset Li(H_2O)_5\cdot(H_2O)_2]\cdot(NO_3)_9\cdot 16.5(H_2O)$ ([Hy-Li]⊂1): Yield: 68% (65 mg), based on Ni. FT-IR data (cm^{-1}): 3859, 3743, 3152, 2959, 1646, 1581, 1508, 1477, 1392, 1327, 1269, 1174, 1116, 1056, 1030, 949, 807, 748, 694. Anal. Calcd. for $C_{128}H_{183}N_{41}O_{66.5}LiP_8Ni_4$: C, 39.94; H, 4.79; N, 14.92. Found: C, 40.12; H, 4.65; N, 14.80.

$[\{Ni_4L_8(H_2O)_8\}\supset 0.25\{Na(H_2O)_5\}\cdot(H_2O)_{5.5}]\cdot(NO_3)_{8.25}\cdot 20(H_2O)$ ([Hy-Na]⊂1): Yield: 61% (59 mg), based on Ni. FT-IR data (cm^{-1}): 3860, 3744, 3146, 2959, 1646, 1581, 1508, 1477, 1392, 1328, 1269, 1181, 1117, 1058, 1030, 949, 808, 748, 694. Anal. Calcd. for $C_{128}H_{189.5}N_{40.25}O_{67.5}Na_{0.25}P_8Ni_4$: C, 39.82; H, 4.95; N, 14.60. Found: C, 40.03; H, 4.72; N, 14.57.

$[\{Ni_4L_8(H_2O)_8\}\supset K(H_2O)_8]\cdot(NO_3)_9\cdot 17(H_2O)$ ([Hy-K]⊂1): Yield: 72% (70 mg), based on Ni. FT-IR data (cm^{-1}): 3860, 3744, 3143, 2958, 1646, 1581, 1510, 1477, 1394, 1328, 1269, 1180, 1117, 1058, 1028, 949, 807, 749, 694. Anal. Calcd. for $C_{128}H_{186}N_{41}O_{68}KP_8Ni_4$: C, 39.33; H, 4.80; N, 14.69. Found: C, 39.22; H, 5.01; N, 14.54.

$[\{Ni_4L_8(H_2O)_8\}\supset Rb(H_2O)_9]\cdot(NO_3)_9\cdot 20(H_2O)$ ([Hy-Rb]⊂1): Yield: 70% (71 mg), based on Ni. FT-IR data (cm^{-1}): 3861, 3745, 3153, 2963, 1646, 1581, 1511, 1477, 1394, 1327, 1269, 1175, 1118, 1058, 1028, 950, 808, 748, 694. Anal. Calcd. for $C_{128}H_{194}N_{41}O_{72}RbP_8Ni_4$: C, 38.18; H, 4.86; N, 14.26. Found: C, 38.37; H, 4.75; N, 13.98.

$[\{Ni_4L_8(H_2O)_8\}\supset Cs(H_2O)_{10}]\cdot(NO_3)_9\cdot 17(H_2O)$ ([Hy-Cs]⊂1): Yield: 69% (70 mg), based on Ni. FT-IR data (cm^{-1}): 3861, 3744, 3145, 2961, 1646, 1578, 1511, 1466, 1394, 1328, 1268, 1176, 1117, 1057, 1028, 950, 807, 748, 694. Anal. Calcd. for $C_{128}H_{190}N_{41}O_{70}CsP_8Ni_4$: C, 38.07; H, 4.74; N, 14.22. Found: C, 37.83; H, 4.77; N, 14.27.

$[\{Co_4L_8(H_2O)_8\}\supset Li(H_2O)_5\cdot(H_2O)_2]\cdot(NO_3)_9\cdot 25(H_2O)$ ([Hy-Li]⊂2): Yield: 52% (52 mg), based on Co. FT-IR data (cm^{-1}): 3860, 3742, 3152, 2959, 1647, 1580, 1508, 1477, 1391, 1325, 1269, 1176, 1116, 1059, 1029, 949, 807, 749, 694. Anal. Calcd. for $C_{128}H_{200}N_{41}O_{75}LiP_8Co_4$: C, 38.40; H, 5.04; N, 14.34. Found: C, 38.63; H, 4.89; N, 14.23.

$[\{Co_4L_8(H_2O)_8\}\supset 0.25\{Na(H_2O)_5\}\cdot(H_2O)_5]\cdot(NO_3)_{8.25}\cdot 27(H_2O)$ ([Hy-Na]⊂2): Yield: 51% (49 mg), based on Co. FT-IR data (cm^{-1}): 3860, 3743, 3146, 2960, 1647, 1580, 1510, 1476, 1392, 1328, 1269, 1180, 1117, 1059, 1030, 949, 807, 748, 694. Anal. Calcd. for $C_{128}H_{189.5}N_{40.25}O_{67.5}Na_{0.25}P_8Co_4$: C, 39.81; H, 4.95; N, 14.60. Found: C, 39.60; H, 4.83; N, 14.43.

$[\{Co_4L_8(H_2O)_8\}\supset K(H_2O)_8]\cdot(NO_3)_9\cdot 23(H_2O)$ ([Hy-K]⊂2): Yield: 69% (69 mg), based on Co. FT-IR data (cm^{-1}): 3861, 3742, 3144, 2958, 1646, 1580, 1510, 1476, 1394, 1329, 1269, 1180, 1117, 1059, 1029, 949, 807, 749, 694. Anal. Calcd. for $C_{128}H_{198}N_{41}O_{74}KP_8Co_4$: C, 38.26; H, 4.97; N, 14.29. Found: C, 38.41; H, 4.70; N, 14.35.

$[\{Co_4L_8(H_2O)_8\}\supset Rb(H_2O)_9]\cdot(NO_3)_9\cdot 27(H_2O)$ ([Hy-Rb]⊂2): Yield: Yield: 65% (67 mg), based on Co. FT-IR data (cm^{-1}): 3860, 3745, 3149, 2960, 1648, 1580, 1510, 1477, 1394, 1327, 1268, 1175, 1118, 1058, 1028, 949, 808, 749, 694. Anal. Calcd. for $C_{128}H_{208}N_{41}O_{79}RbP_8Co_4$: C, 37.01; H, 5.05; N, 13.82. Found: C, 37.13; H, 4.96; N, 14.03.

$[\{Co_4L_8(H_2O)_8\}\supset Cs(H_2O)_{10}]\cdot(NO_3)_9\cdot 25(H_2O)$ ([Hy-Cs]⊂2): Yield: 66% (69 mg), based on Co. FT-IR data (cm^{-1}): 3860, 3746, 3146, 2959, 1649, 1581, 1510, 1472, 1394, 1328, 1269, 1175, 1117, 1058, 1028, 949, 807, 748, 694. Anal. Calcd. for $C_{128}H_{206}N_{41}O_{78}CsP_8Co_4$: C, 36.75; H, 4.96; N, 13.73. Found: C, 36.92; H, 4.87; N, 14.00.

Phase purity for all the [Hy-A]⊂**1** and [Hy-A]⊂**2** systems were confirmed by powder X-ray diffraction analysis (Fig. S1 and S2, ESI).

Crystallography

Reflections were collected on a Bruker Smart Apex Duo diffractometer at 100 K using MoKα radiation (λ = 0.71073 Å) for the crystals of **1**, **2**, [Hy-A]⊂**1** and [Hy-A]⊂**2**. Structures were refined by full matrix least squares against F^2 using all data (SHELX).[2] Crystallographic data for all these compounds are listed in Table S1 (ESI). All non-hydrogen atoms were refined anisotropically, if not stated otherwise. Hydrogen atoms were constrained in geometric positions to their parent atoms. The phenyl rings were thermally disordered in all the cases, hence the atom positions of the disordered groups were freely refined isotropically over two positions using similar distances and similar U-restraints. The water molecules encapsulated within the **1**, **2**, [Hy-A]⊂**1** and [Hy-A]⊂**2** were also disordered. Hence their occupancies and numbers were fixed using the SUMP command. The nitrate ions in all these structures were disordered along with the solvated molecules at the packing cavities. Hence, these were treated as diffuse contributions to the overall scattering and removed by the SQUEEZE/PLATON. In case of [Hy-Li]⊂**1**, [Hy-Rb]⊂**1** , [Hy-Cs]⊂**1**, [Hy-Rb]⊂**2** and [Hy-Cs]⊂**2**, the most disagreeable reflection outliers were removed using OMIT command. We have also provided a disorder model (a partial squeeze data) for the nitrate ions in **1** showing their probable sites of occupation at the unit cell lattice.

Ferroelectric and Dielectric Measurements

To determine the dielectric and ferroelectric properties, the powdered samples of all the compounds were compacted in the form of discs (of approximately 10 mm diameter and 1mm thickness). The compacted discs were subsequently electroded using aluminium adhesive foils for both ferroelectric and dielectric measurements. The frequency dependent dielectric characteristics for **1**, **2**, [Hy-A]⊂**1** and [Hy-A]⊂**2** at various temperatures were measured using the Novocontrol, Dielectric Spectrometer. The ferroelectric hysteresis loop in **1**, [Hy-A]⊂**1** and [Hy-A]⊂**2** were measured by using Sawyer-Tower circuit. Both polarizations and fatigue studies were recorded using hysteresis loop analyser (TF Analyser 2000, aixACCT Germany). Time-dependent leakage current was measured dynamically during the hysteresis loop measurements. It was recorded for various applied voltage steps using the TF analyser.

Calculation of Dipole Moment

The dipole moment of **1** was obtained by performing single-point ONIOM calculations by using the Gaussian 09 program.[3] The cationic cage segment was considered as low layer while the encapsulated H_2O, solvates and nitrate anions were selected as high layer to perform ONIOM calculation. The high layer was optimized by DFT methods (B3lyp/6-31g) and semi-empirical method (PM6) was used for the lower layer.

Table S1: Details of crystallographic data collection and structure refinements for **1**, **2**, [Hy-A]⊂**1**and [Hy-A]⊂**2** systems.

Compound	**1**	[Hy-Li]⊂**1**	[Hy-Na]⊂**1**
Chemical formula	$C_{128}H_{204}N_{40}O_{74}P_8Ni_4$	$C_{128}H_{183}LiN_{41}O_{66.50}P_8Ni_4$	$C_{128}H_{189.50}Na_{0.25}N_{40.25}O_{67.50}P_8Ni_4$
Formula weight	3969.90	3849.68	3860.53
Temperature (K)	100(2)	100(2)	100 (2)
Crystal system	Tetragonal	Tetragonal	Tetragonal
Space group	I422	I422	I422
a (Å); α (°)	24.810(2); 90	24.222(7); 90	24.399(7); 90
b (Å); β(°)	24.810(2); 90	24.222(7); 90	24.399(7);90
c (Å); γ (°)	17.809(15); 90	17.620(4); 90	17.576(5); 90
V (Å^3); Z	10963(2); 2	10337(6) ; 2	10463(6); 2
ρ (calc.) mg m^{-3}	1.203	1.237	1.225
μ mm^{-1}	0.481 (Mo K$_\alpha$)	0.505 (Mo K$_\alpha$)	0.500 (Mo K$_\alpha$)
2θ$_{max}$ (°)	56	56	45
R(int)	0.0822	0.1493	0.0471
Completeness to θ	100 %	99.9 %	99.7 %
Data / param.	6848 / 218	6535 / 220	3427 / 220
GOF	1.066	0.996	1.081
R1 [F>4σ(F)]	0.0668	0.0693	0.0520
wR2 (all data)	0.2478	0.2468	0.1664
max. peak/hole (e.Å^{-3})	0.455 /-0.260	0.544/-0.290	0.636/-0.253
Compound	[Hy-K]⊂**1**	[Hy-Rb]⊂**1**	[Hy-Cs]⊂**1**
Chemical formula	$C_{128}H_{186}KN_{41}O_{68}P_8Ni_4$	$C_{128}H_{194}RbN_{41}O_{72}P_8Ni_4$	$C_{128}H_{190}CsN_{41}O_{70}P_8Ni_4$
Formula weight	3908.87	4027.30	4038.71
Temperature	100(2)	100(2)	100(2)
Crystal system	Tetragonal	Tetragonal	Tetragonal
Space group	I422	I422	I422
a (Å); α (°)	24.382(2); 90	24.570(8); 90	24.462(6); 90
b (Å); β(°)	24.382(2);90	24.570(8);90	24.462(6);90
c (Å); γ (°)	17.522(3); 90	17.699(7); 90	17.608(5); 90
V (Å^3); Z	10417(3); 2	10685(8); 2	10537(6); 2
ρ (calc.) mg m^{-3}	1.246	1.252	1.273
μ mm^{-1}	0.522 (Mo K$_\alpha$)	0.719 (Mo K$_\alpha$)	0.668 (Mo K$_\alpha$)
2θ$_{max}$ (°)	56	56	56
R(int)	0.0795	0.1900	0.0844
Completeness to θ	100 %	99.9 %	99.9 %
Data / param.	6531 / 224	6634 / 224	6711 / 224
GOF	1.036	0.963	1.032
R1 [F>4σ(F)]	0.0495	0.0618	0.0446
wR2 (all data)	0.1602	0.1943	0.1368
max. peak/hole (e.Å^{-3})	0.747 / -0.228	0.286 /-0.320	0.442 /-0.502

Compound	**2**	[Hy-Li]⊂**2**	[Hy-Na]⊂**2**
Chemical formula	$C_{128}H_{208}Co_4N_{40}O_{76}P_8$	$C_{128}H_{200}LiN_{41}O_{75}P_8Co_4$	$C_{128}H_{202.5}Na_{0.25}N_{40.25}O_{74}P_8Co_4$
Formula weight	4006.81	4003.70	3978.52
Temperature	100(2)	100(2)	100(2)
Crystal system	Tetragonal	Tetragonal	Tetragonal
Space group	I422	I422	I422
a (Å); α (°)	24.556(4); 90	24.507(6); 90	24.524(12); 90
b (Å); β(°)	24.556(4);90	24.507(6);90	24.524(12);90
c (Å); γ (°)	17.680(3); 90	17.716(6); 90	17.661(8); 90
V (Å^3); Z	10661(4); 2	10640(6); 2	10622(12); 2
ρ (calc.) mg m^{-3}	1.248	1.250	1.244
μ mm^{-1}	0.454 (Mo K$_{\alpha}$)	0.454 (Mo K$_{\alpha}$)	0.455 (Mo K$_{\alpha}$)
2θ$_{max}$ (°)	56	56	50
R(int)	0.0860	0.2162	0.2054
Completeness to θ	100 %	100 %	99.9 %
Data / param.	6641 / 195	6661 / 173	4705 / 172
GOF	1.058	0.964	0.947
R1 [F>4σ(F)]	0.0861	0.0876	0.0879
wR2 (all data)	0.3228	0.3234	0.3072
max. peak/hole (e.Å^{-3})	0.765 /-0.354	0.594 /-0.396	0.781/-0.298
Compound	[Hy-K]⊂**2**	[Hy-Rb]⊂**2**	[Hy-Cs]⊂**2**
Chemical formula	$C_{128}H_{198}KN_{41}O_{74}P_8Co_4$	$C_{128}H_{208}RbN_{41}O_{79}P_8Co_4$	$C_{128}H_{206}CsN_{41}O_{78}P_8Co_4$
Formula weight	4017.84	4154.29	4183.72
Temperature	100(2)	100(2)	100(2)
Crystal system	Tetragonal	Tetragonal	Tetragonal
Space group	I422	I422	I422
a (Å); α (°)	24.404(4); 90	24.651(3); 90	24.580(3); 90
b (Å); β(°)	24.404(4);90	24.651(3);90	24.580(3);90
c (Å); γ (°)	17.589(3); 90	17.773(2); 90	17.611(3); 90
V (Å^3); Z	10476(4); 2	10801(3); 2	10640(3); 2
ρ (calc.) mg m^{-3}	1.274	1.277	1.306
μ mm^{-1}	0.481 (Mo K$_{\alpha}$)	0.674 (Mo K$_{\alpha}$)	0.625 (Mo K$_{\alpha}$)
2θ$_{max}$ (°)	56	56	56
R(int)	0.1837	0.0623	0.0444
Completeness to θ	100 %	99.9 %	99.9 %
Data / param.	6564 / 201	6750 / 201	6612 / 201
GOF	0.977	1.044	1.028
R1 [F>4σ(F)]	0.0692	0.0503	0.0375
wR2 (all data)	0.2402	0.1623	0.1133
max. peak/hole (e.Å^{-3})	0.322 /-0.262	0.391 /-0.307	0.411 /-0.266

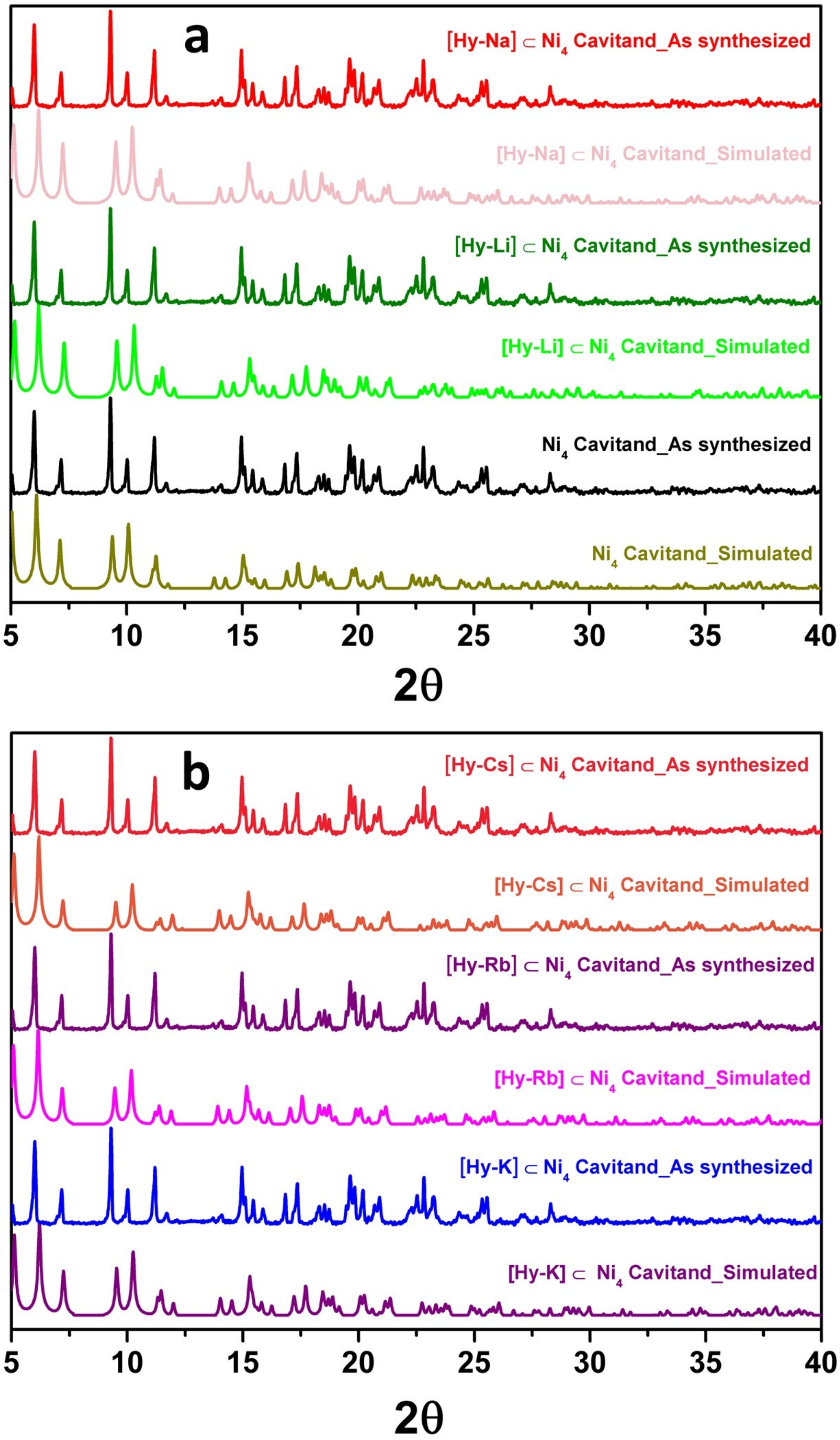

Fig. S1. Powder X-ray diffraction (PXRD) profiles of Ni_4 cavitand (**1**) and {[Hy-A]⊂**1**}.

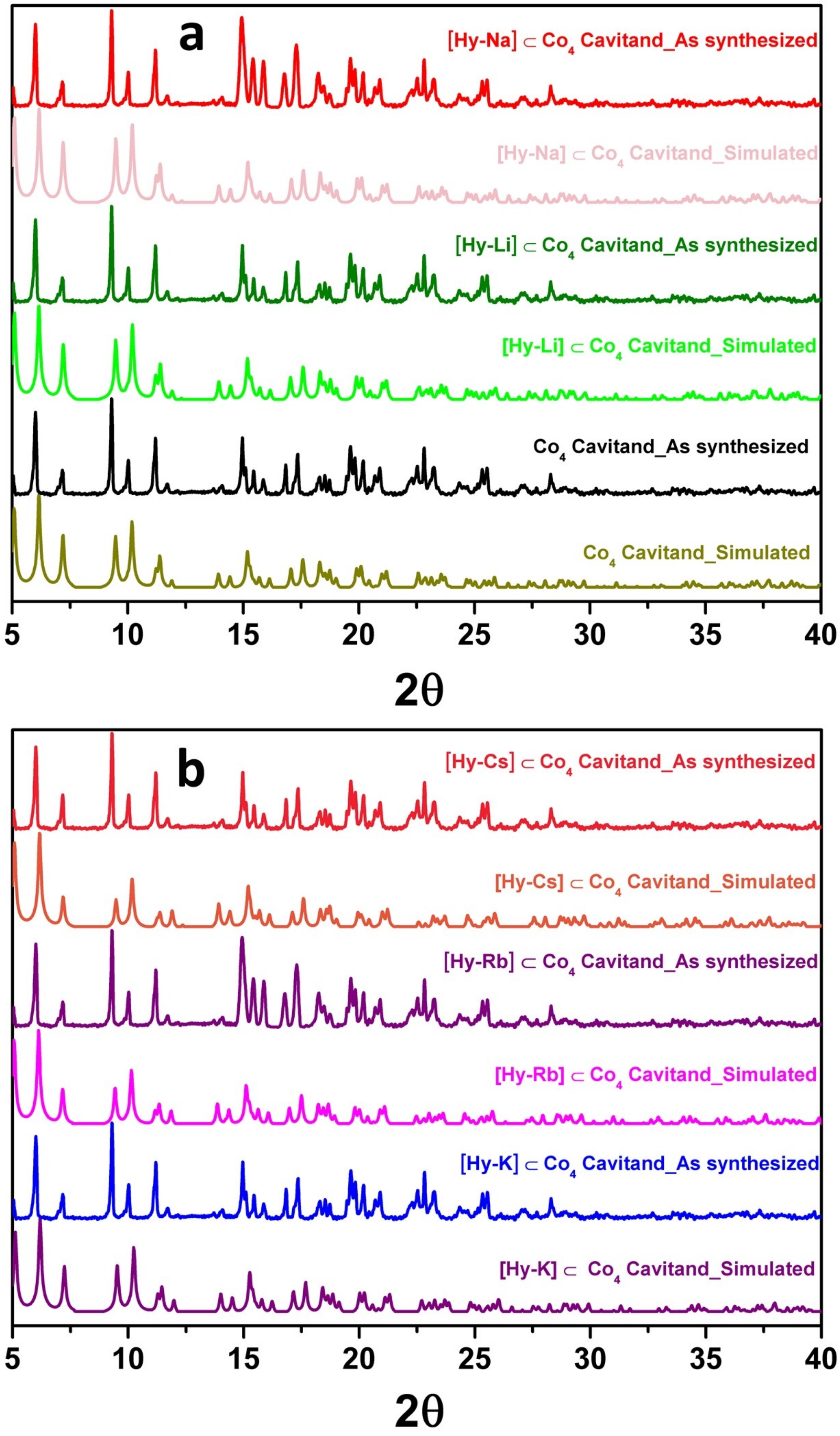

Fig. S2. Powder X-ray diffraction (PXRD) profiles of Co_4 cavitand (**2**) and {[Hy-A]⊂**2**}.

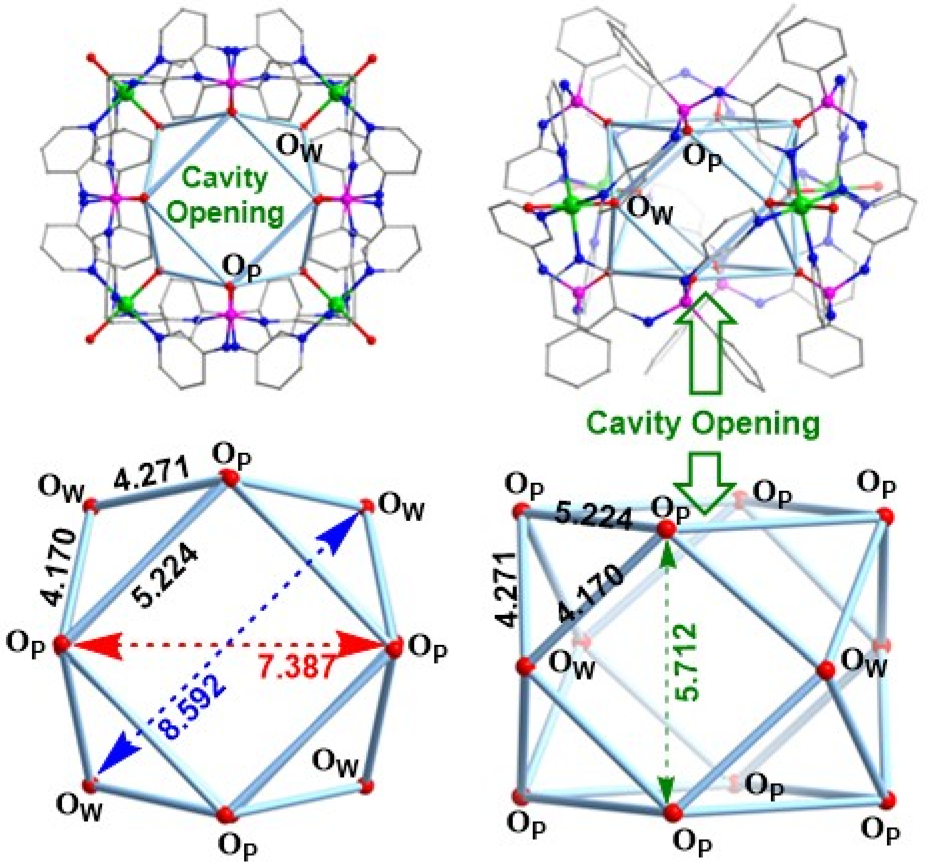

Fig. S3. View of the intrinsic void in**1** and the metric parameters associated with the cavity.

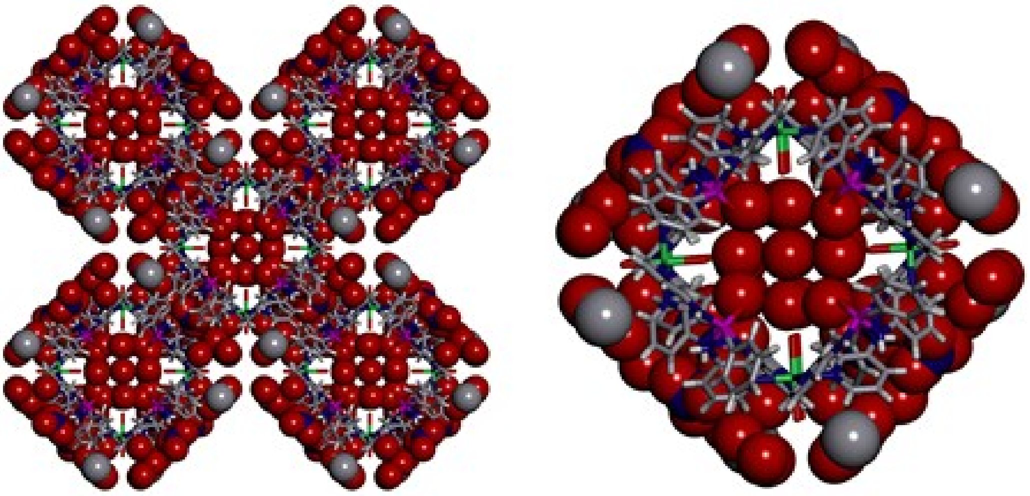

Fig. S4. Packing structure of **1**; the encapsulated polar guest solvents as well as the solvents and nitrate anions in the packing cavity were shown in the space-fill representation (colour code: C, grey; N, blue; O, red; P, purple; Ni, light-green; H, white).

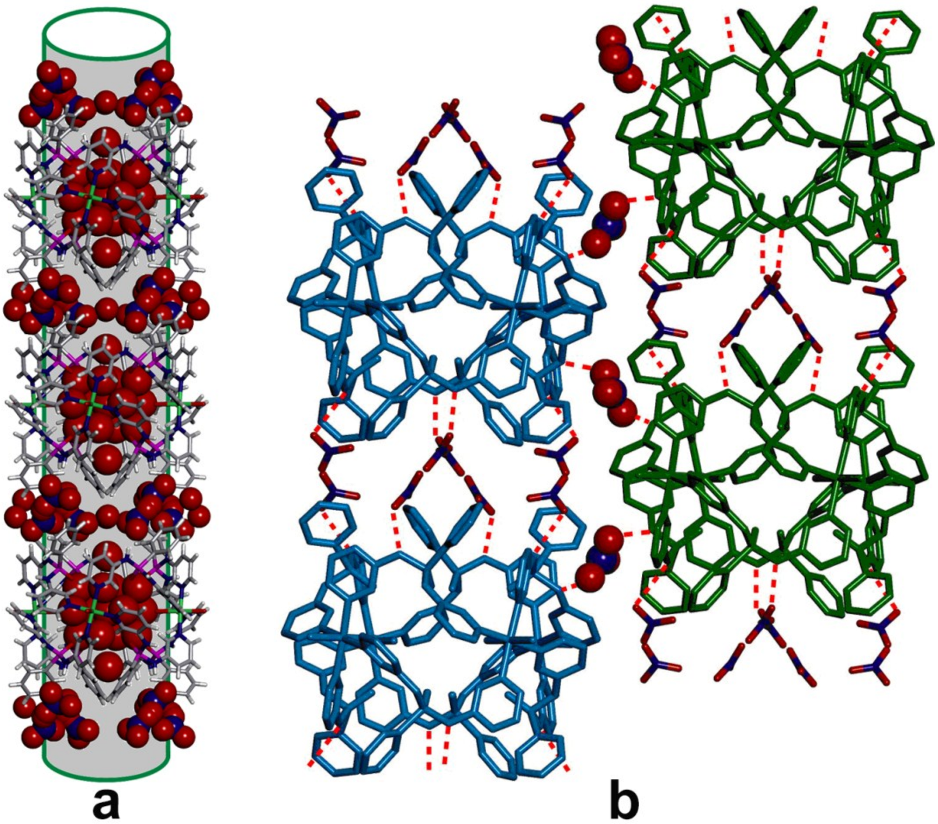

Fig. S5. (a) View of the contiguous 1D-channel like structure in **1**along the c-axis showing the eclipsed arrangement of the Ni$_4$-cavitand;connection between the cages along the 1d-channel structure were provided by disordered nitrate anions and extrinsic solvates via H-bonding. (b) Linkage between the adjacent 1D-channels via the interaction of the additional nitrate ions (shown in the space filled representation).

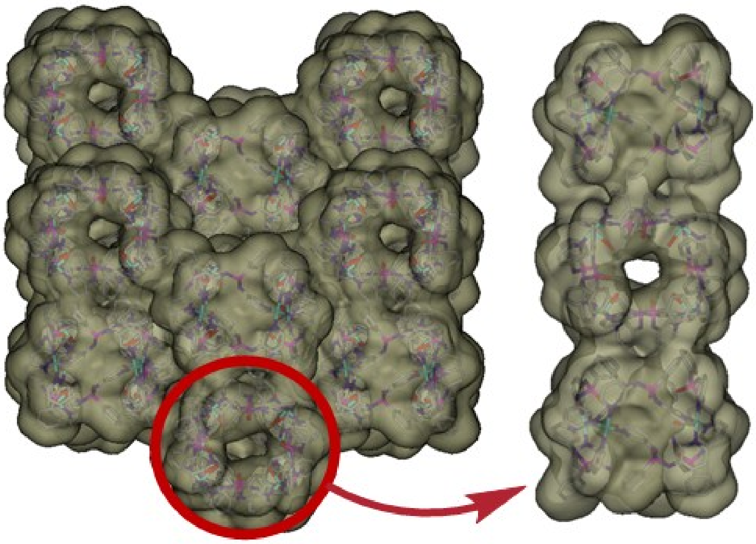

Fig. S6. Packing arrangement of the earlier reported Cu$_4$ cavitand and view of the interrupted channel along the c-axis.[1]

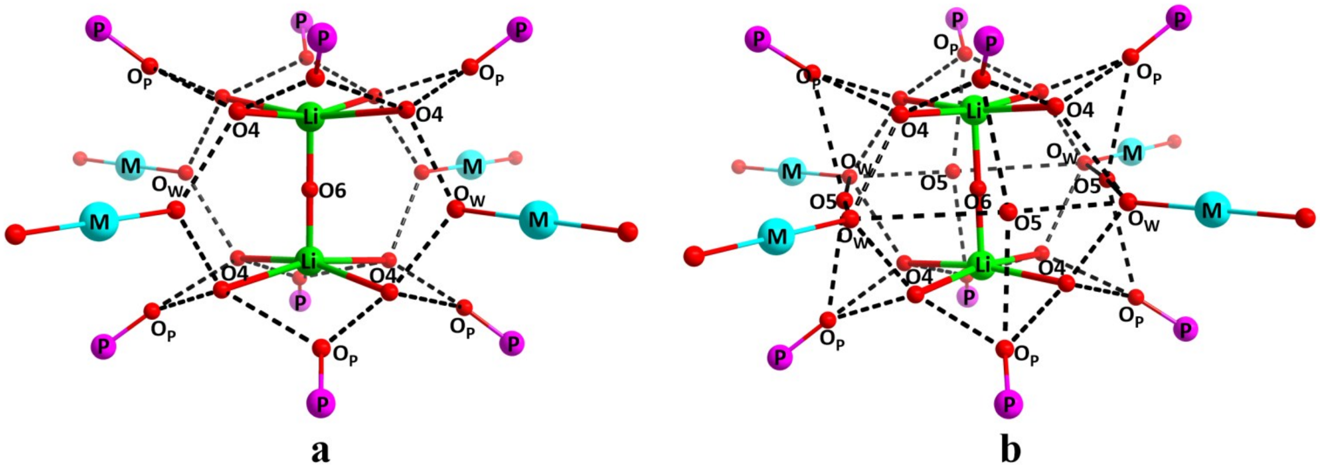

Fig. S7. (a)View of the disordered $[Li(H_2O)_5]^+$motif in [Hy-Li]⊂**1**and [Hy-Li]⊂**2**alongwith its H-bonding interactions. (b)Location of the additional encapsulated water molecules (O5) in [Hy-Li]⊂**1**and [Hy-Li]⊂**2**and their interactions with the host framework. (M= Ni^{2+} or Co^{2+})

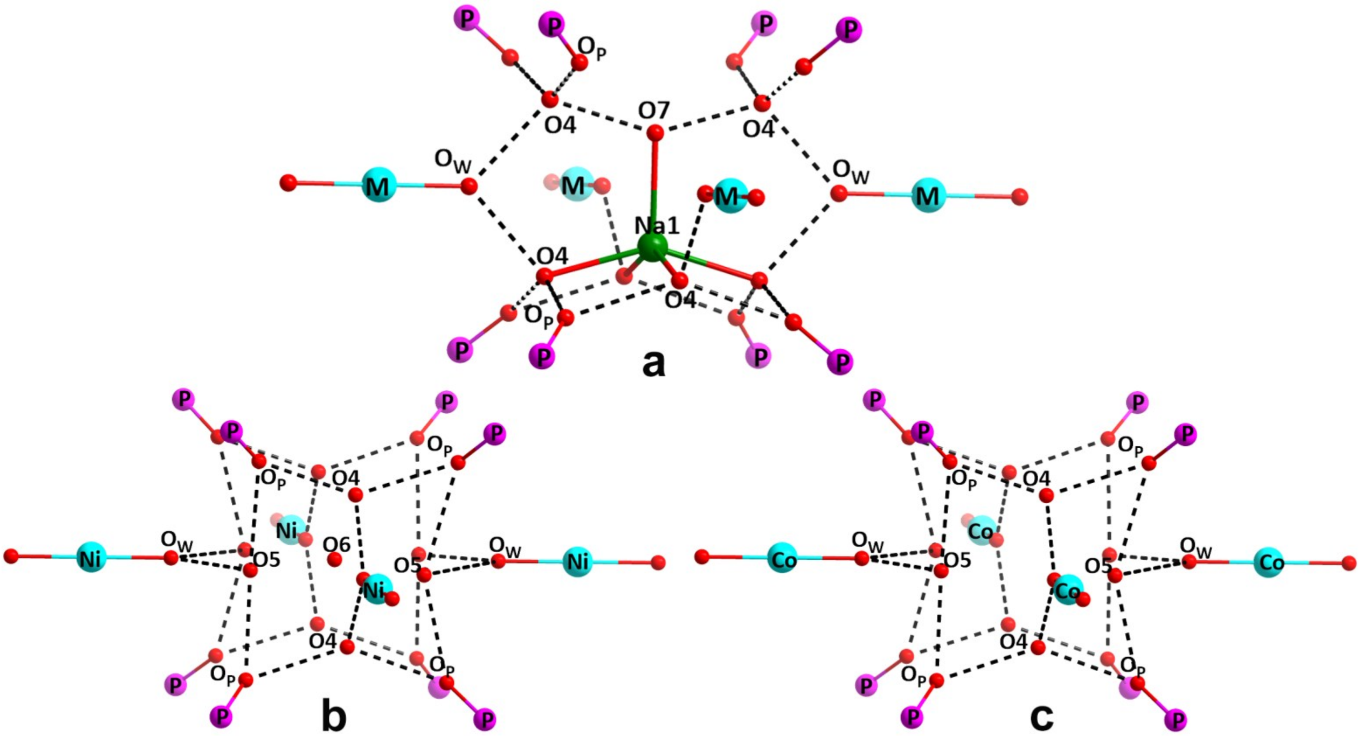

Fig. S8. View of the two distinct guest environments in [Hy-Na]⊂**1** and [Hy-Na]⊂**2**. (a) One of the disordered segment of the$[Na(H_2O)_5]^+$ guest and its H-bonding with the host framework**1** or **2**(M= Ni^{2+} or Co^{2+}). (b) View of the additional water cluster (made up of O4, O5 and O6) encapsulated inside [Hy-Na]⊂**1**.(c) View of the additional water cluster (made up of O4 and O5) encapsulated inside [Hy-Na]⊂**2**.

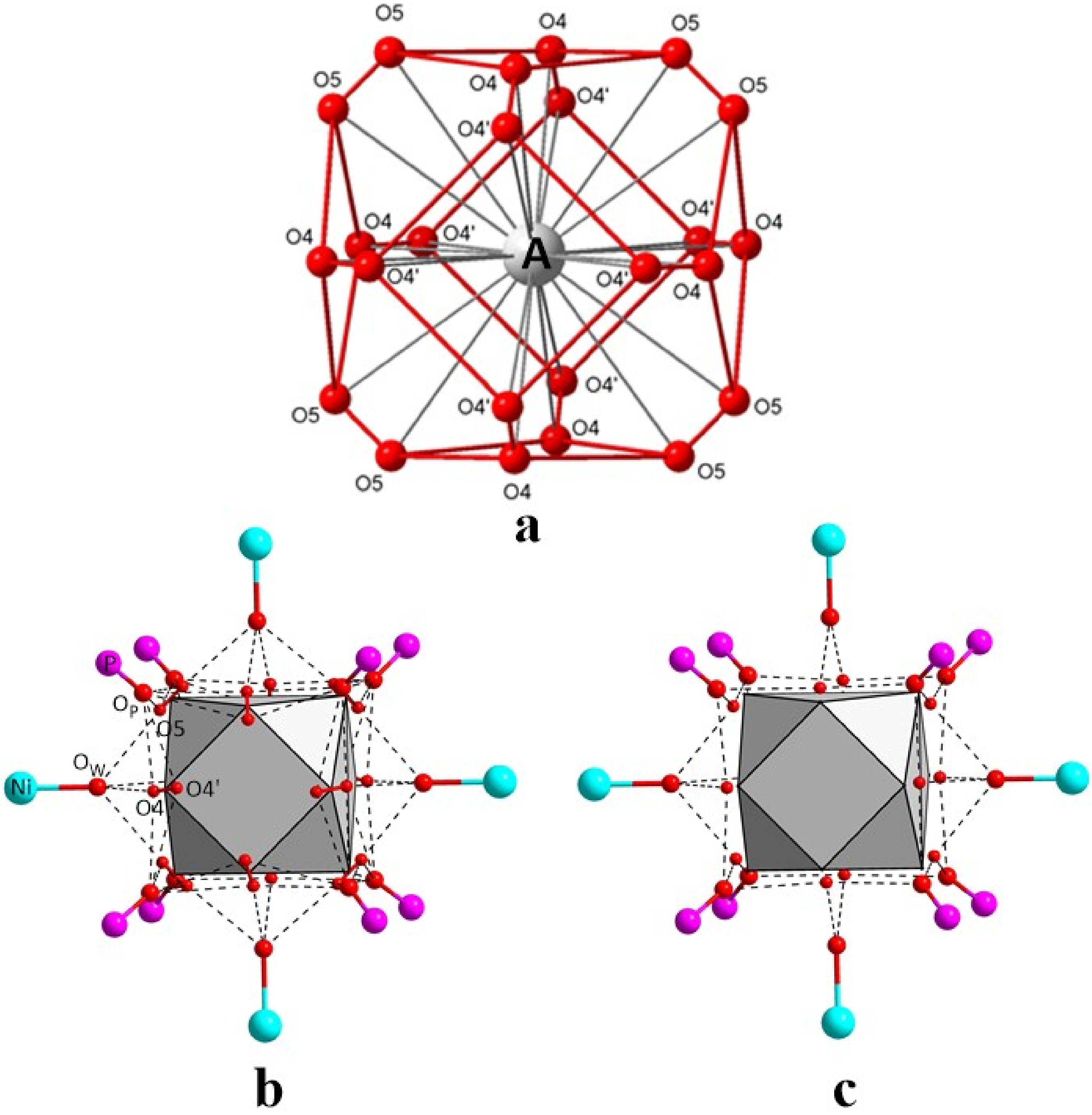

Fig. S9. View of the hydration sphere around the K$^+$/Rb$^+$/Cs$^+$ ions in {[Hy-A]⊂**1**} and {[Hy-A]⊂**2**}. (a) The 24 vertex truncated cube made up of symmetry equivalent O4, O4′ and O5 atoms in the disordered state. (b) and (c) shows the formation of a cuboctahedralcoordination around the alkali metal ion via the omission of one of the disordered sites of O4/O4′ and O5 atoms.

Table S2: Refinements of {[Hy-A]⊂**1** (A=K^+, Rb^+, and Cs^+) complexes with varying coordination numbers

A	A(H_2O)$_n$	Occupancy factor			Isotropic displacement parameter (U)						R1	Sum of occupancy factors	
		O4	O4'	O5	U(O)	U(M)	U(Ni)	U(O1)	U(O2)	U(O3)		O4+O4'	O4+O5
K	6	0.53	0.03	0.19	0.049	0.078	0.054	0.070	0.055	0.082	0.055	0.562	0.716
	7	0.60	0.05	0.22	0.058	0.078	0.054	0.070	0.055	0.082	0.052	0.655	0.822
	8	0.68	0.07	0.25	0.067	0.078	0.054	0.070	0.055	0.082	0.050	0.749	0.927
	9	0.75	0.09	0.28	0.076	0.078	0.054	0.070	0.055	0.082	0.048	0.842	1.030
	10	0.82	0.12	0.31	0.084	0.078	0.054	0.069	0.055	0.082	0.048	0.935	1.133
	11	0.89	0.14	0.35	0.093	0.078	0.054	0.069	0.055	0.081	0.049	1.028	1.234
	12	0.96	0.17	0.38	0.101	0.078	0.054	0.069	0.054	0.081	0.051	1.123	1.333
Rb	6	0.44	0.12	0.19	0.027	0.057	0.055	0.063	0.054	0.086	0.069	0.560	0.626
	7	0.50	0.15	0.23	0.038	0.057	0.055	0.063	0.054	0.086	0.066	0.648	0.727
	8	0.56	0.17	0.26	0.048	0.057	0.055	0.063	0.053	0.085	0.064	0.737	0.827
	9	0.63	0.20	0.30	0.058	0.057	0.055	0.063	0.053	0.085	0.063	0.825	0.926
	10	0.69	0.22	0.34	0.067	0.057	0.055	0.063	0.052	0.085	0.062	0.914	1.025
	11	0.75	0.25	0.37	0.077	0.057	0.055	0.063	0.052	0.085	0.061	1.003	1.125
	12	0.82	0.27	0.41	0.087	0.057	0.055	0.063	0.052	0.084	0.061	1.091	1.227
Cs	6	0.39	0.17	0.19	0.020	0.043	0.048	0.054	0.047	0.072	0.058	0.564	0.577
	7	0.45	0.21	0.22	0.028	0.043	0.048	0.054	0.047	0.072	0.054	0.654	0.669
	8	0.51	0.24	0.26	0.036	0.043	0.048	0.054	0.046	0.072	0.050	0.744	0.764
	9	0.57	0.27	0.29	0.044	0.043	0.048	0.054	0.046	0.072	0.047	0.832	0.860
	10	0.63	0.29	0.33	0.052	0.043	0.048	0.054	0.046	0.071	0.045	0.919	0.956
	11	0.68	0.32	0.37	0.059	0.043	0.048	0.054	0.046	0.071	0.045	1.004	1.056
	12	0.74	0.34	0.41	0.067	0.043	0.048	0.054	0.046	0.071	0.047	1.088	1.156

This table lists refinements of K^+, Rb^+ and Cs^+ complexes with varying coordination numbers of A (alkali metal ion) ranging from 6 to 12. This was done by fixing the sum of occupancy factors of O4, O4' and O5 and at the same time refine them with a combined isotropic displacement parameter U(O) (column highlighted in yellow) in order to suppress correlations between occupancy factors and U-values. For comparison, U-values of A, Ni and other O-atoms are listed alongside R1. Columns O4+O4' and O4+O5 give the sum of occupancy factors of the two sites. These cannot exceed a value of 1.0 since this would bring two coordination sites into too close contact (values in excess of 1.0 are highlighted in red). Comparison of the resulting parameters of the various runs shows that the coordination number tends to increases from K^+ to Cs^+. While it is difficult to extract definite numbers from these values, coordination numbers of 8, 9 and 10 for K^+, Rb^+ and Cs^+, respectively, appear to be in good agreement with listed values (rows highlighted in yellow).

Table S3: Refinements of {[Hy-A]⊂**2** (A=K^+, Rb^+, and Cs^+) complexes in their most suitable hydration numbers.

A	$A(H_2O)_n$	Occupancy factor			Isotropic displacement parameter (U)						R1	Sum of occupancy factors	
		O4	O4'	O5	U(O)	U(M)	U(Co)	U(O1)	U(O2)	U(O3)		O4+O4'	O4+O5
K	8	0.65	0.10	0.25	0.067	0.069	0.050	0.059	0.068	0.097	0.067	0.747	0.899
Rb	9	0.34	0.48	0.31	0.054	0.042	0.046	0.053	0.048	0.093	0.054	0.818	0.643
Cs	10	0.59	0.27	0.39	0.050	0.032	0.031	0.047	0.034	0.035	0.040	0.857	0.985

Table S4: List of A-O* distances and O-O distances between coordinated water and oxygen atoms of the {[Hy-A]⊂**1** (A=K^+, Rb^+, and Cs^+) host-guest assemblies (in Å).

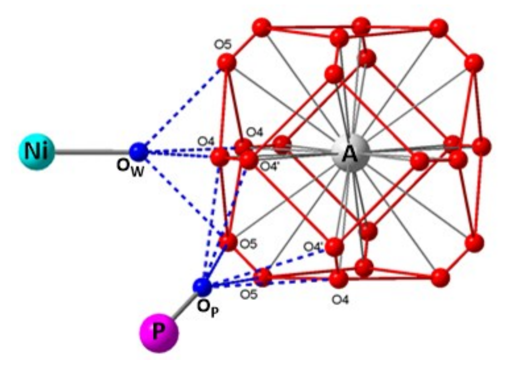	**A**	A-O4	A-O4'	A-O5	O_P-O4	O_P-O4'	O_P-O5	O_W-O4	O_W-O5
	K	3.05	3.12	3.09	2.73 2.81	2.72 2.80	2.86 2.89	2.64	2.55
	Rb	3.18	3.27	3.29	2.73 2.80	2.66 2.87	2.81 2.87	2.71	2.63
	Cs	3.27	3.29	3.35	2.77 2.79	2.70 2.89	2.78 2.89	2.69	2.66

*The A-O distances show a slight increase from K^+ to Cs^+, while O-O distances are fairly similar for the different hydrated guest, and are in the appropriate range for hydrogen bonding.

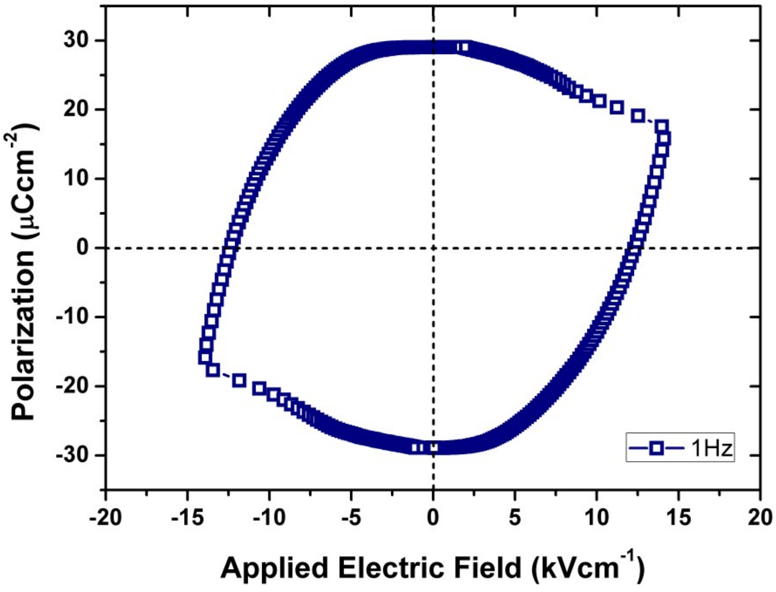

Fig. S10. Ferroelectric hysteresis loop of **1** at 1 Hz at room temperature.

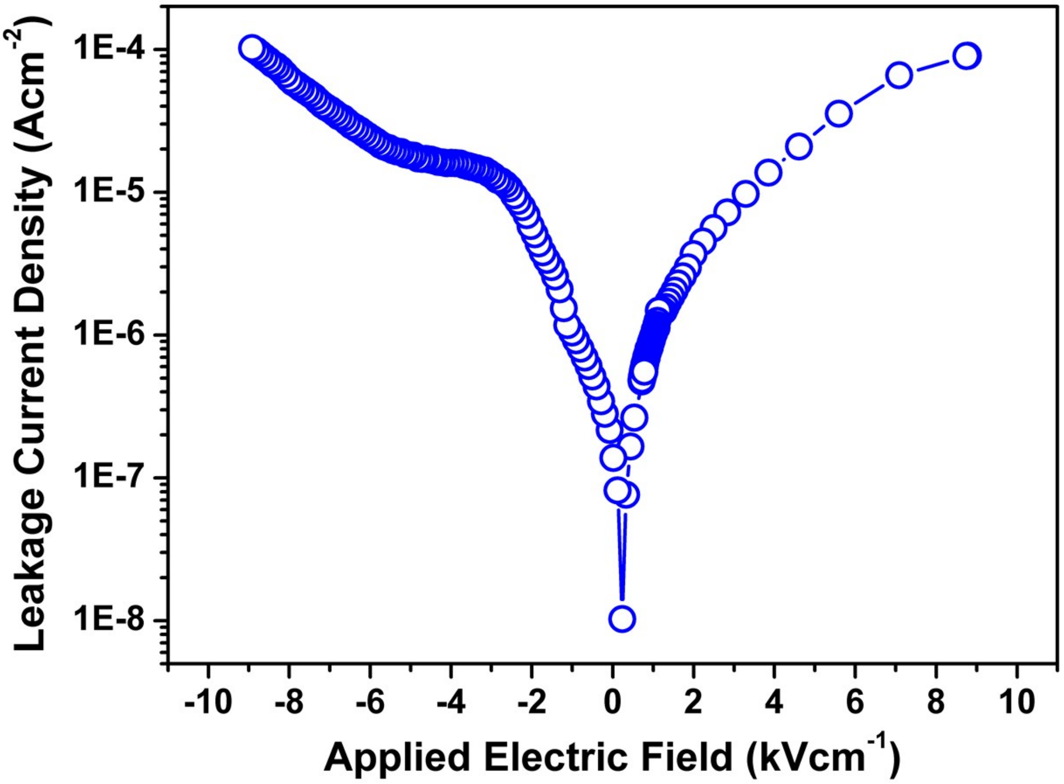

Fig. S11. Plot of the Leakage current density vs applied electric field for **1**.

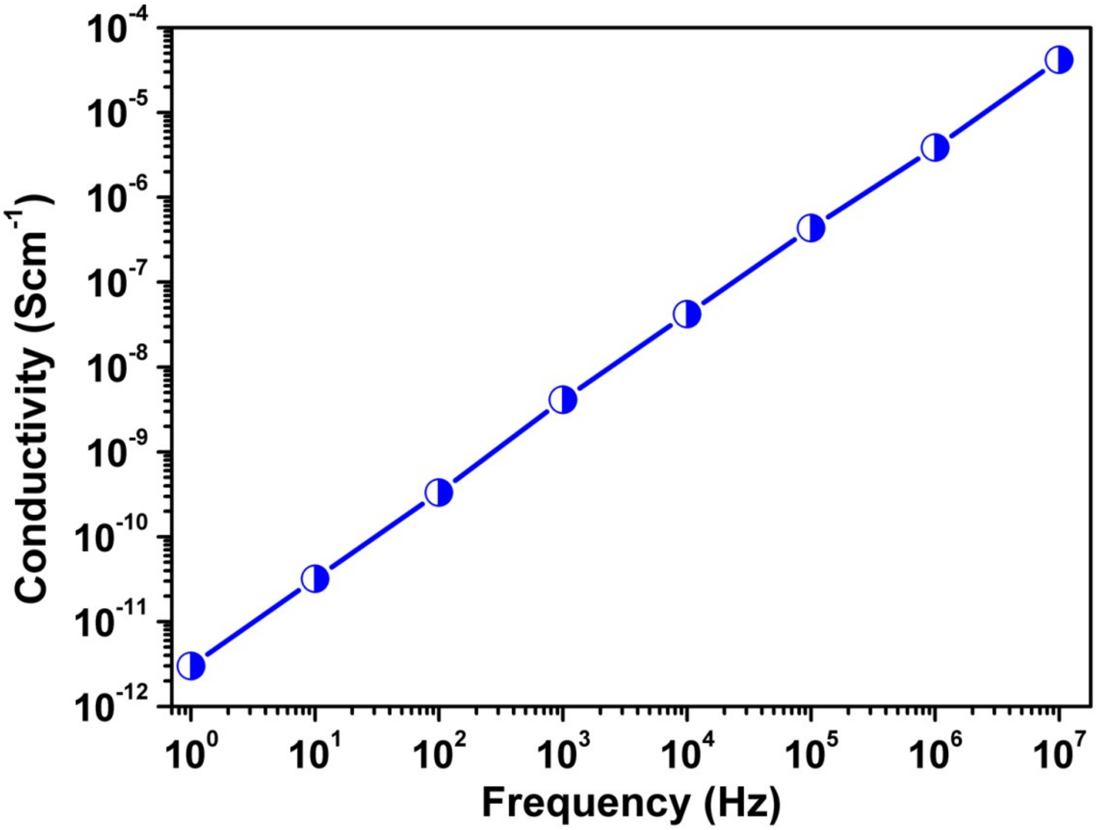

Fig. S12. Frequency dependent plot of the conductivity of **1** at 30˚C.

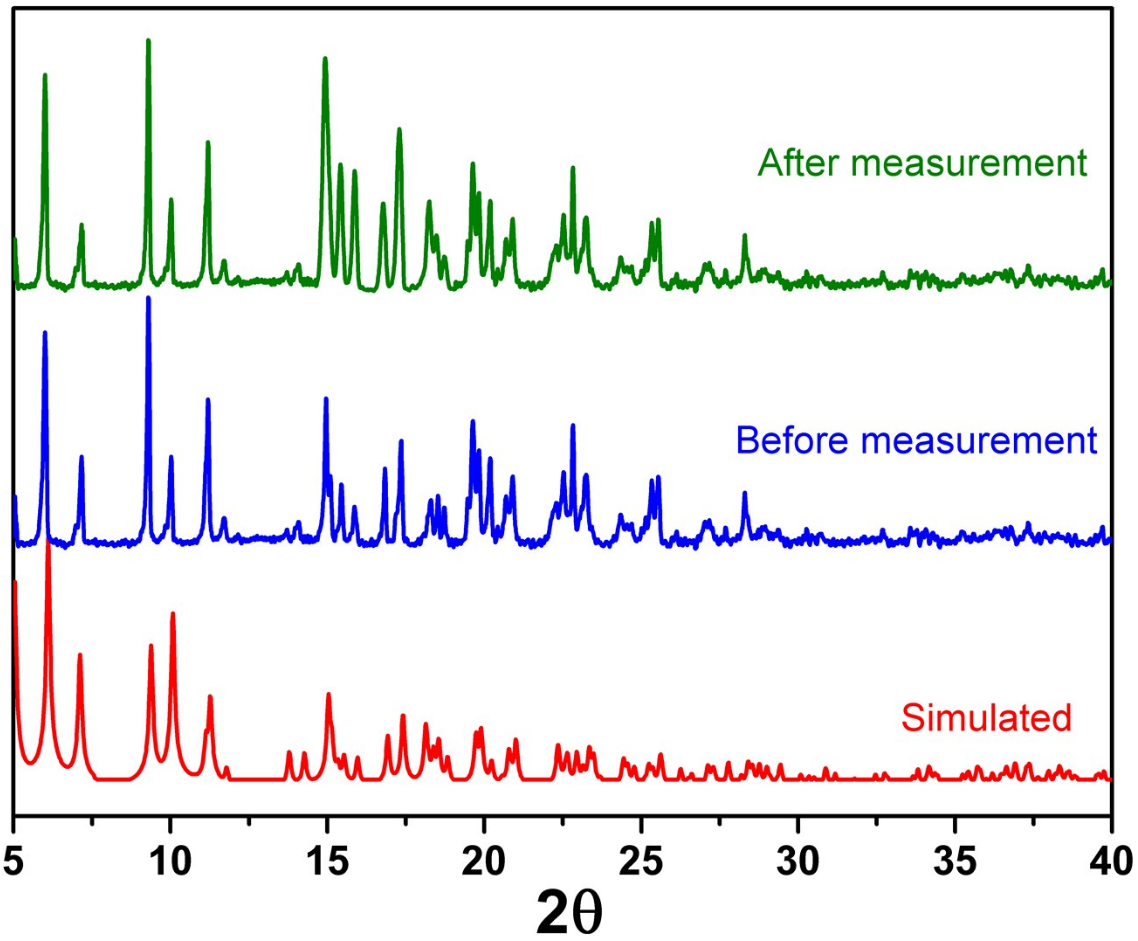

Fig. S13. Comparison of the PXRD patterns of the disc of **1** before and after ferroelectric measurements.

Table S5: Single-point ONIOM Calculation on **1** (using b3lyp/6-31g: hf/pm6 basis set).

System	Dipole Moment (Debye)
Cage+Anion+Solvent	66.3870
Cage+Anion	26.1042

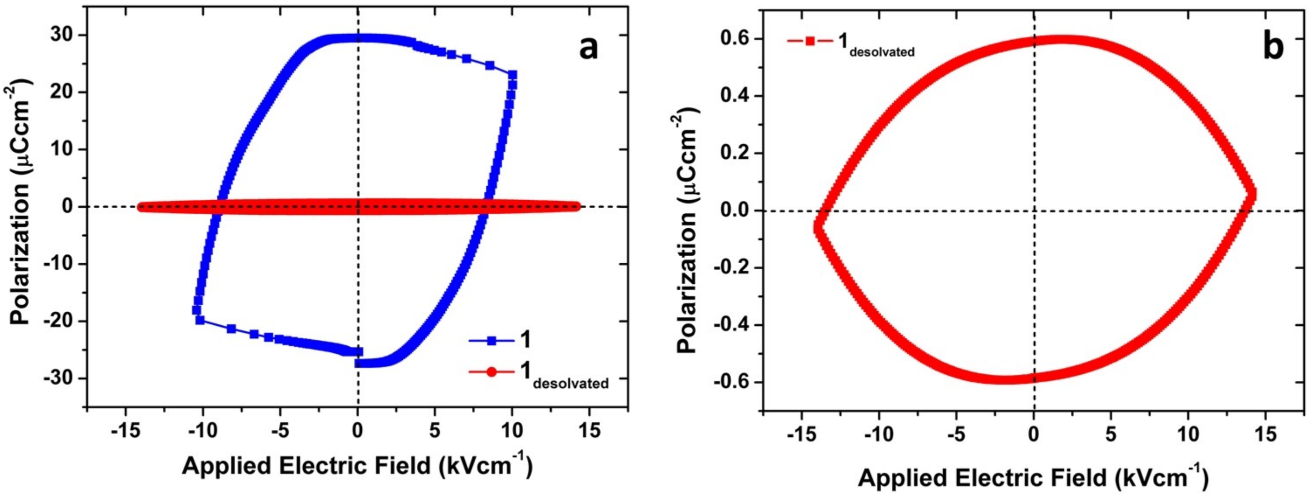

Fig. S14. Comparison of the P-E loops for **1** (a) and **1$_{desolvated}$** (a & b).

Table S6: Saturation Polarization (P_s) and Coercive Field (E_c) value of selected organic/metal-organic ferroelectric materials reported till date.

S.No.	**Materials**	**P_s (μCcm^{-2}); Temperature (K)**	**E_c (kVcm^{-1})**	**Reference**
1.	Croconic Acid	21; RT	14	4
2.	Vinylidene fluoride (VDF) oligomer	13; RT	1200	5, 6
3.	Copolymer P(VDF-TrFE)	8; RT	500	5, 7
4.	Nylon-11	5; RT	600	5
5.	$NaNO_2$	10; 140K	5	5
6.	KH_2PO_4(KDP)	5	0.1	5
7.	$HdabcoReO_4$	16; RT	>30	5
8.	Triglycinesulphate (TGS)	3.8; 220K	0.9	5, 8
9.	Rochelle Salt	0.25; 276K	0.2	5, 9
10.	Guanidinium perchlorate	8.4; RT	8.7	10
11.	Guanidiniumtetrafluoroborate	8.5; RT	11.4	10
12.	Diisopropylammonium bromide	23; 422K	5	11
13.	Diisopropylammonium Chloride	8.9; 418K	9	12
14.	$[InC_{16}H_{11}N_2O_8]\cdot(H_2O)_{1.5}$	1.64; 297K	1.65	13
15.	$\{[Cu_2L_4(H_2O)_2]\cdot(ClO_4)_4\cdot(H_2O)_5\cdot(CH_3OH)\}_\infty$ *	1.8; RT	16	1
16.	$(\{[CuL^1_2(H_2O)_2]\cdot(NO_3)_2\cdot(H_2O)_{1.5}\cdot(CH_3OH)\}_\infty)$ **	21.79; RT	5.9	14

*L= $PhPO(NH^3Py)_2$ ** L^1=$PhPO(NH^4Py)_2$ {where, ^{3}Py= 3-Pyridyl; ^{4}Py=4-Pyridyl}

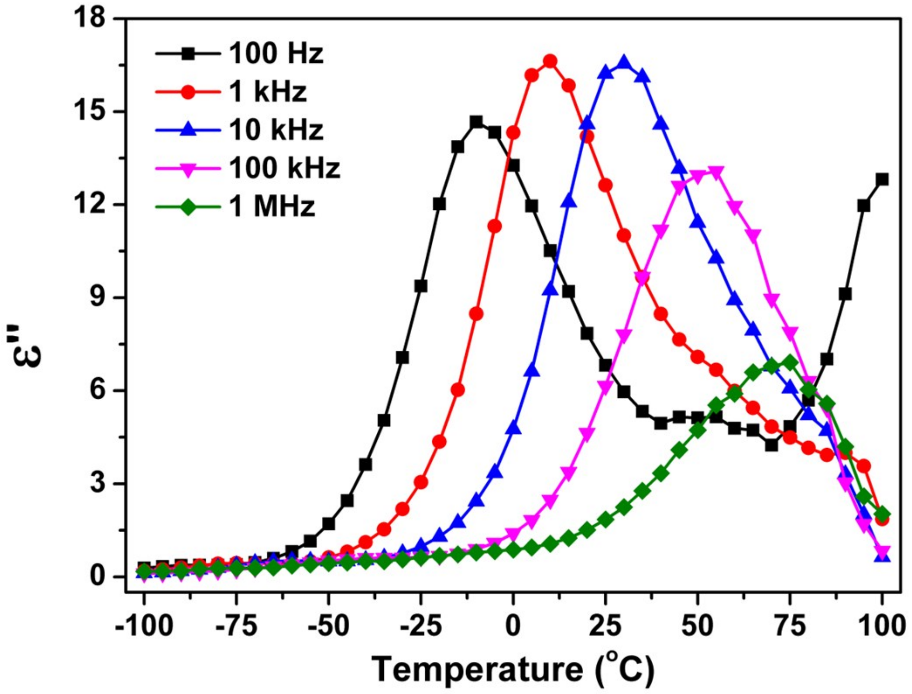

Fig. S15. Temperaturedependence of the imaginary part (ε’’) of dielectric permittivity of **1**.

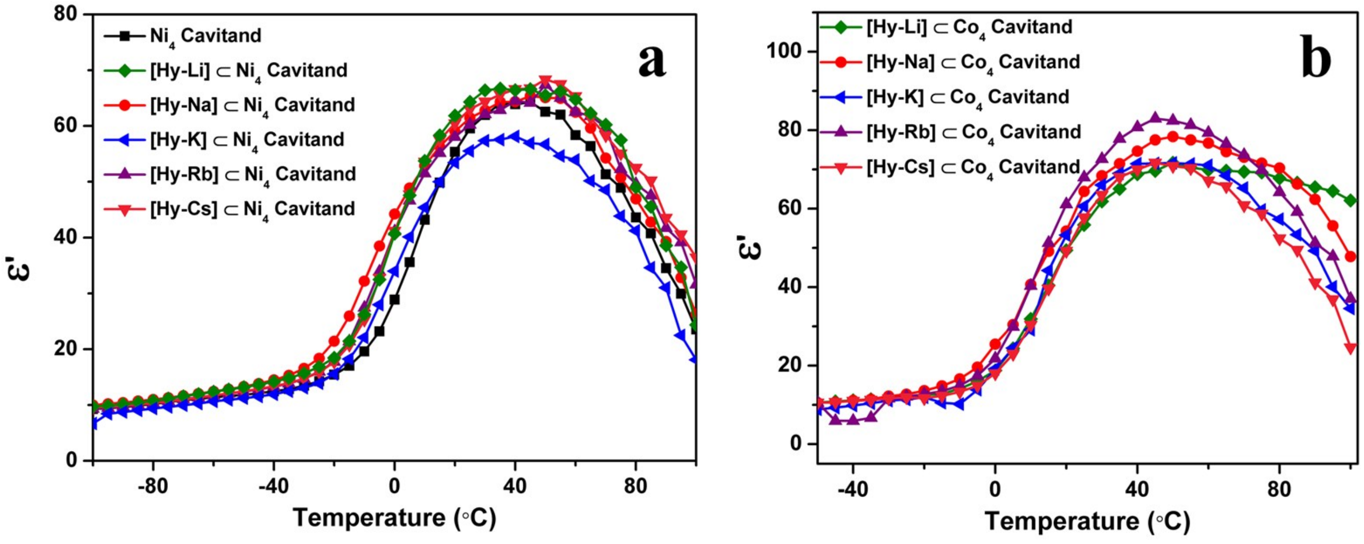

Fig. S16. Temperature dependent real part of dielectric constants for (a) {[Hy-A]⊂**1**} and (b) {[Hy-A]⊂**2**} systems at 1kHz.

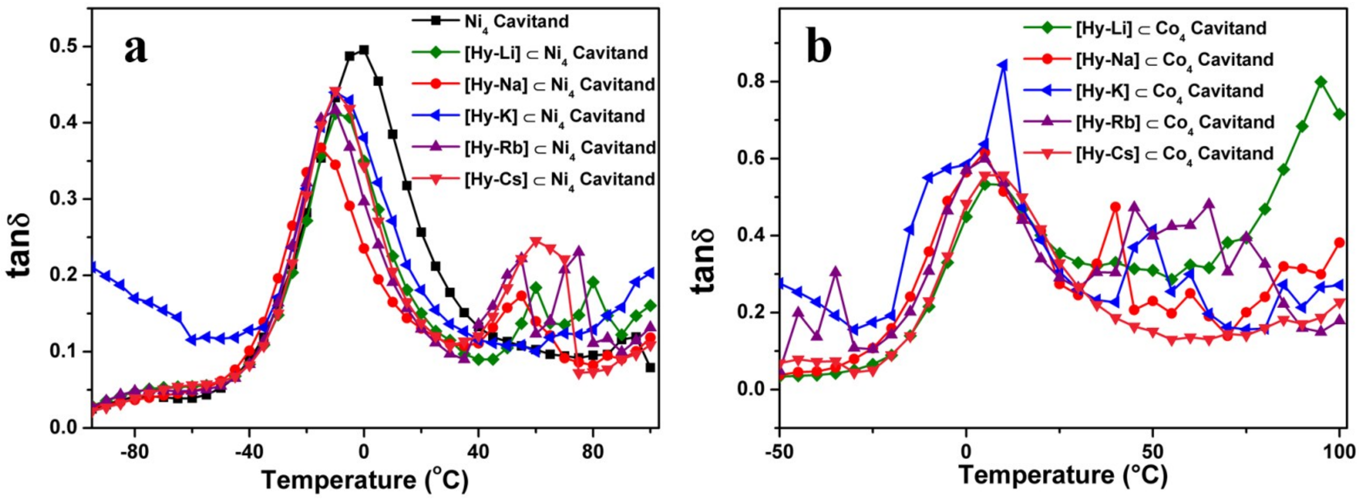

Fig. S17. Temperature dependence of the dielectric loss for (a) {[Hy-A]⊂**1**} and (b) {[Hy-A]⊂**2**}at 1 kHz.

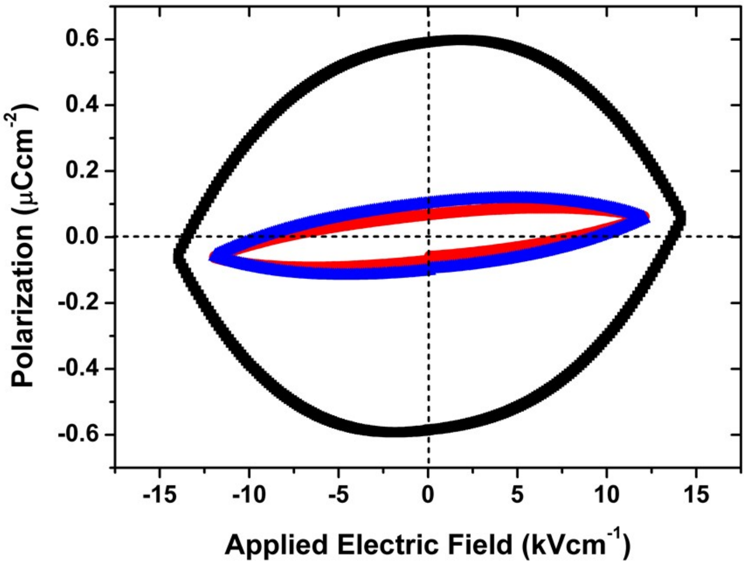

Fig. S18. P-E loop of the desolvated sample of **1** (black), {[Hy-Li]⊂**1**} (blue) and {[Hy-Cs]⊂**1**} (red).

Table S7: The P_r loss (%) data obtained from ferroelectric fatigue measurement cavitands.

Host-Guest Assembly	**P_r loss (in %) after 10^5 switching cycles**	
	Ni_4-series	**Co_4**-series
M_4*	6.423	--
[Hy-Li]⊂**M_4**	9.029	0.1858
[Hy-Na]⊂**M_4**	--	2.099
[Hy-K]⊂**M_4**	21.1102	0.7023
[Hy-Rb]⊂**M_4**	21.099	3.177
[Hy-Cs]⊂**M_4**	34.7173	12.5014

*For the sake of simplicity $(H_2O)_9\subset M_4$ is given only as M_4 throughout the manuscript and supporting information

References

1. A. K. Srivastava, B. Praveenkumar, I. K. Mahawar, P. Divya, S. Shalini and R. Boomishankar, *Chem. Mater.*, 2014, **26**, 3811-3817.
2. G. M. Sheldrick, *Acta Crystallogr. C*, 2015, **71**, 3-8.
3. M. Frisch, G. Trucks, H. Schlegel, *GAUSSIAN 03*, *Revision B. 05*, Gaussian Inc., Wallingford, CT, 2004.
4. S. Horiuchi, Y. Tokunaga, G. Giovannetti, S. Picozzi, H. Itoh, R. Shimano, R. Kumai and Y. Tokura, *Nature*, 2010, **463**, 789-792.
5. S. Horiuchi and Y. Tokura, *Nat. Mater.* 2008, **7**, 357-366.
6. K. Noda, K. Ishida, A. Kubono, T. Horiuchi, H. Yamada and K. Matsushige, *J. Appl. Phys.*, 2003, **93**, 2866-2870.
7. T. Furukawa, *Phase Trans.*, 1989, **18**, 143-211.
8. M. Szafrański, A. Katrusiak and G. J. McIntyre, *Phys. Rev. Lett.*, 2002, **89**, 215507.
9. S. Hoshino, T. Mitsui, F. Jona and R. Pepinsky, *Phys. Rev.*, 1957, **107**, 1255.
10. M. Szafrański, *J. Phys. Chem. B*, 2011, **115**, 8755-8762.
11. D.-W. Fu, H.-L. Cai, Y. Liu, Q. Ye, W. Zhang, Y. Zhang, X.-Y. Chen, G. Giovannetti, M. Capone, J. Li and R. G. Xiong, *Science*, 2013, **339**, 425-428.
12. D.-W. Fu, W. Zhang, H. L. Cai, J. Z. Ge, Y. Zhang and R. G. Xiong, *Adv. Mater.*, 2011, **23**, 5658-5662.
13. L. Pan, G. Liu, H. Li, S. Meng, L. Han, J. Shang, B. Chen, A. E. Platero-Prats, W. Lu, X. Zou and R.-W. Li, *J. Am. Chem. Soc.*, 2014, **136**, 17477-17483.
14. A. K. Srivastava, P. Divya, B. Praveenkumar and R. Boomishankar, *Chem. Mater.*, 2015, **27**, 5222-5229.